

The Laplace transform to describe bounded inhomogeneous waves

Nico F. Declercq^{a)} and Joris Degrieck

Soete Laboratory, Department of Mechanical Construction and Production, Faculty of Engineering,
Ghent University, Sint Pietersnieuwstraat 41, 9000 Gent, Belgium

Oswald Leroy

Interdisciplinary Research Center, KULeuven Campus Kortrijk, E. Sabbelaan 53, 8500 Kortrijk, Belgium

(Received 23 February 2004; accepted for publication 11 April 2004)

The inhomogeneous waves theory deals with plane waves having complex valued wave vectors and with their superposition to form bounded beams. Since infinite inhomogeneous plane waves cannot be formed experimentally, verifications of the theory have to be performed using bounded inhomogeneous waves. In this paper we clarify how a bounded inhomogeneous wave is described as a superposition of inhomogeneous waves. This is done by applying the Laplace transform. The paper also shows from a theoretical point of view why bounded inhomogeneous waves behave like infinite inhomogeneous waves in numerous experiments. © 2004 Acoustical Society of America. [DOI: 10.1121/1.1756672]

PACS numbers: 43.20.Bi, 43.20.El, 43.35.Pt [ADP]

Pages: 51–60

I. INTRODUCTION

From the moment infinite inhomogeneous waves have made their entry in the 1980's, they have been used in the study of the propagation and the scattering of sound. They gained sympathy because of their ability to describe—often better than pure infinite homogeneous plane waves—critical phenomena like the generation of Leaky Rayleigh waves. An extensive survey on the properties of infinite inhomogeneous plane waves can be found in the literature.^{1–4} While infinite inhomogeneous plane waves are often studied in the context of their superposition to form bounded beams,^{5–7} perhaps even more interesting is the theoretical and experimental study of individual inhomogeneous waves. A lot of experiments are reported that confirm theoretical predictions of the behavior of inhomogeneous waves while interacting with interfaces.^{2,8–11} The interesting part of these confirmations is the fact that infinite inhomogeneous waves can only be approached experimentally within a limited spatial interval, depending on the apparatus that is used experimentally.⁸ The overall experimentally generated wave is in fact a bounded inhomogeneous wave, being a chopped and smoothed version of the theoretical infinite inhomogeneous wave. The importance of bounded inhomogeneous waves, as compared with bounded Gaussian beams, is the fact that they contain the inhomogeneity features of inhomogeneous waves (i.e., the exponential decay of the amplitude along the wave front) and are hence capable of stimulating more efficiently critical phenomena such as leaky Rayleigh waves or leaky Lamb waves than Gaussian beams. Furthermore, this resemblance with infinite inhomogeneous waves is the reason why at incidence angles that correspond to the stimulation of critical phenomena, a strong beam shift occurs^{2,8–11} to the reflected beam as the principle effect, which is different from the Schoch effect (the creation of two reflected lobes with a null

zone in between) that occurs if Gaussian beams are used. In what follows, we investigate bounded inhomogeneous waves in terms of infinite inhomogeneous plane waves, using a numerical technique that has never been applied before in such a context, namely the Laplace transform. In fact, as far as we know, no reports exist at all where bounded inhomogeneous waves are described in terms of infinite inhomogeneous plane waves.

Whenever the expression “profile” is used in this text, it refers to the normalized particle displacement amplitude profile. Further below, we will consider the oblique incidence of a bounded inhomogeneous wave at an interface ($X', Z' = 0$); see Fig. 1. The profile of this bounded beam can be compared with the profile of the reflected beam if one considers the amplitude distribution along an axis X (see Fig. 1) that coincides with the wave front and for theoretical simplicity has the same origin as the fixed (X', Z') coordinate system. The latter enables us to compare for example possible shifts of the reflected profile along the X -axis with respect to the incident profile.

II. INFINITE INHOMOGENEOUS PLANE WAVES IN A NUTSHELL

For the reader who is not familiar with the theory of infinite inhomogeneous waves, a first glimpse is offered in this section. Anyone who needs to get to know more about this theory is invited to read Refs. 1, 3–4, 6–7.

If a “plane wave solution” having an amplitude A , polarization \mathbf{P} , wave vector \mathbf{k} and angular frequency ω ,

$$A\mathbf{P}\exp(i\mathbf{k}\cdot\mathbf{r}-i\omega t) \quad (1)$$

is entered into the wave equation for viscoelastic media, then it can be shown that the dispersion relation must hold:

$$\mathbf{k}\cdot\mathbf{k} = \left(\frac{\omega}{\nu} + i\alpha_0\right)^2 = \frac{\omega^2}{(\bar{\nu})^2}, \quad (2)$$

^{a)}Electronic mail: NicoF.Declercq@ugent.be

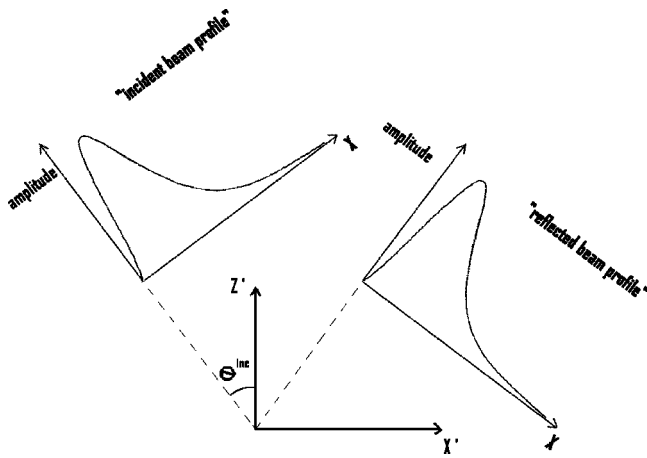


FIG. 1. Schematic of the different coordinate systems. The reflection interface coincides with the X' -axis. The incident beam profile is described along a rotated X' -axis, denoted by X , perpendicular to the propagation direction. The reflected beam profile is also described along a rotated X' -axis, denoted by the same symbol X . Hence, it is possible to compare the profile of the incident beam with that of the reflected beam in a diagram where the amplitude is depicted as a function of the “common” X axis. For convenience, we suppose that the X -axis for both incident and reflected beams has the same origin as the (X', Z') coordinate system.

in which ν is the phase velocity of traditional infinite homogeneous harmonic plane waves, $\bar{\nu}$ is often called “the complex wave velocity” and α_0 is the intrinsic damping coefficient. Therefore in general the wave vector \mathbf{k} can be complex valued, whence

$$\mathbf{k} = \mathbf{k}_1 + i\mathbf{k}_2; \quad \mathbf{k}_1, \mathbf{k}_2 \in \mathfrak{R}^3 \quad (3)$$

and

$$\mathbf{k}_2 = \boldsymbol{\alpha} + \boldsymbol{\beta}, \quad \text{with } \boldsymbol{\beta} \perp \mathbf{k}_1 \text{ and } \boldsymbol{\alpha} \parallel \mathbf{k}_1. \quad (4)$$

The vector \mathbf{k}_1 is called the propagation wave vector. The vector $\boldsymbol{\beta}$ is called the inhomogeneity vector while $\boldsymbol{\alpha}$ is called the damping vector. In many publications the opposite sign for $\boldsymbol{\beta}$ in (4) can be found, but it is more convenient in this outline to use a positive sign. In order to prevent confusion with other papers, we will describe physical problems in terms of the imaginary part of the wave vector, i.e., k_2 , therefore the sign convention of $\boldsymbol{\beta}$ will have no influence on

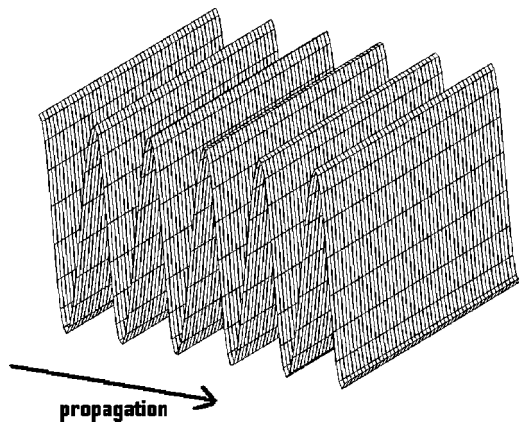


FIG. 2. An infinite pure plane wave (undamped). The amplitude along the wave front remains constant, as well as the amplitude along the propagation direction.

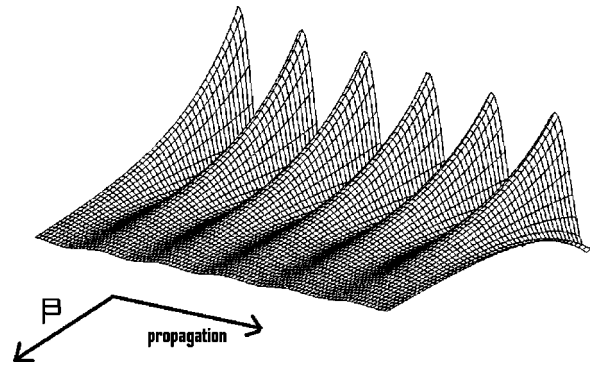


FIG. 3. An infinite inhomogeneous wave (undamped). The amplitude along the wave front decays exponentially down the inhomogeneity vector $\boldsymbol{\beta}$ [according to its definition in (4)]. The amplitude remains constant along the propagation direction.

these discussions. If (3) and (4) are entered in (2), one finds

$$\mathbf{k}_1 \cdot \mathbf{k}_2 = k_1 \alpha = \frac{\omega}{\nu} \alpha_0 \quad (5)$$

and

$$(k_1)^2 - (\alpha)^2 - (\beta)^2 = \left(\frac{\omega}{\nu}\right)^2 - (\alpha_0)^2. \quad (6)$$

Relations (5) and (6) are called the dispersion equations. Due to (5), the damping vector can only exist if there is intrinsic visco-elastic damping in the media. Furthermore, its value depends not only on the intrinsic damping α_0 , but also on the inhomogeneity vector $\boldsymbol{\beta}$. Typical waves (1) are depicted in Figs. 2–4. In the context of what follows, it must be stressed that waves like (1) have a wave front that extends to infinity, i.e., such waves are not bounded in space.

The term infinite inhomogeneous plane waves in the current paper stands for “plane waves” (1) having a complex valued wave vector and a real valued frequency. The polarization will be complex too, but this fact has no influence on the amplitude distribution in space, and is not highlighted here.

Whenever an infinite inhomogeneous plane wave interacts with a plane interface between two media, continuity of the component of \mathbf{k} along the interface is required. This is called the generalized Snell–Descartes law.

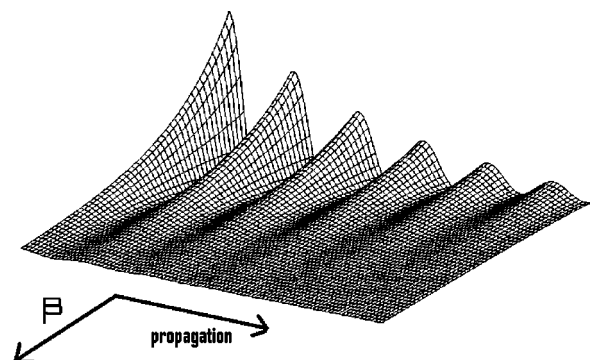


FIG. 4. The same as in Fig. 3, except that there is now damping, therefore the amplitude also decays exponentially along the propagation direction.

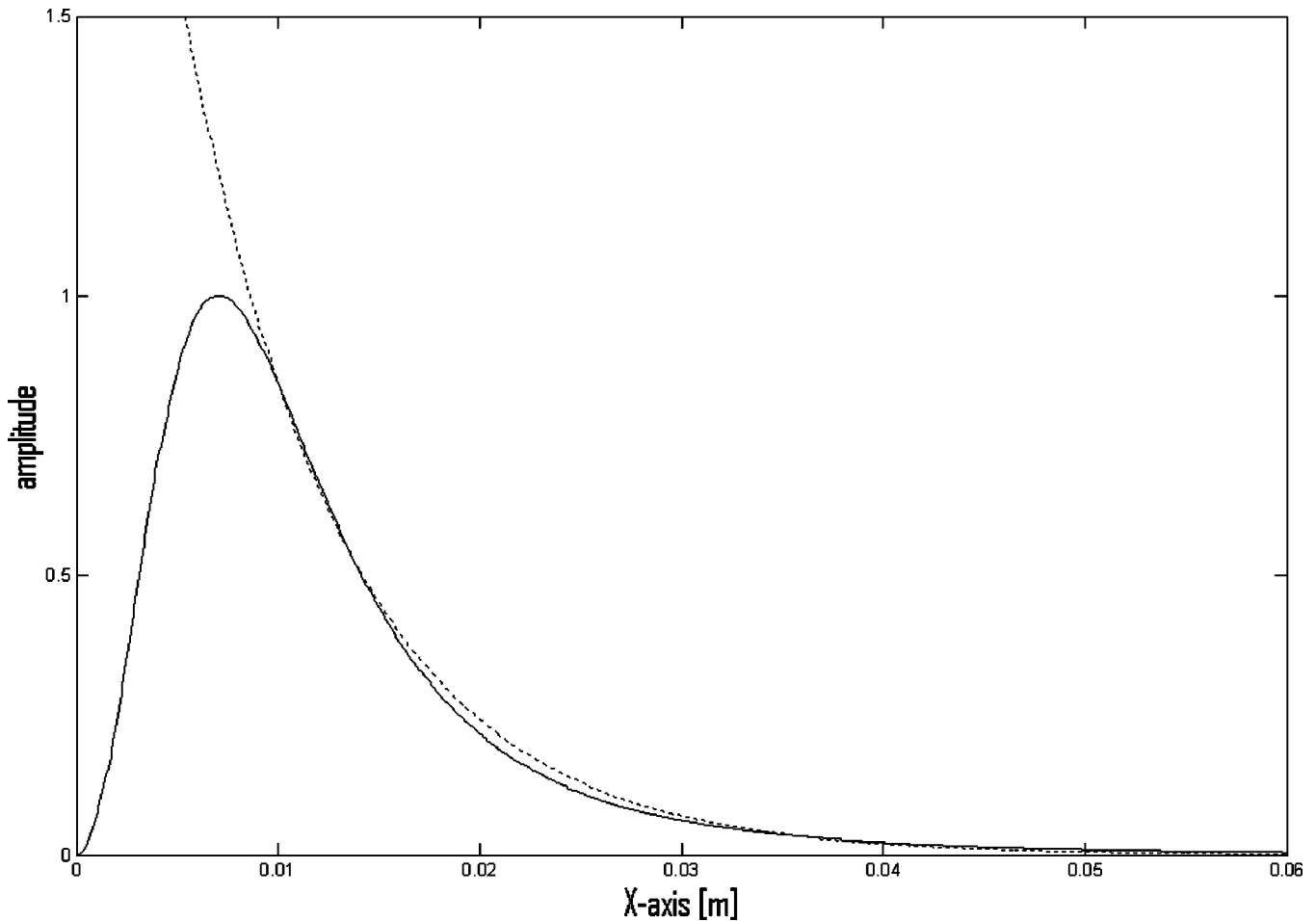


FIG. 5. Solid line: the exact profile (11). Dotted line: the profile of an infinite inhomogeneous wave having an inhomogeneity 125/m.

III. CLASSICAL BOUNDED BEAM FORMATION IN TERMS OF THE FOURIER THEORY

As this method is so widely known, we limit the discourse to a short description in words. In the Fourier theory, a bounded beam profile in X -space (consider Fig. 1) is transformed into $k_{1,x}$ -space by means of the discrete Fourier transform. The amplitudes that correspond to each $k_{1,x}$ value are then attributed to a plane wave having a wave vector component $k_{1,x}$ and another component $k_{1,z}$ that is found as a function of $k_{1,x}$ and the dispersion relation for pure plane waves, i.e. (6) for $\alpha = \beta = 0$. Physically this means that the bounded beam whose profile is considered in the discrete Fourier transform, is built up by means of infinite plane waves all traveling in different directions and having amplitudes determined by that discrete Fourier transform. The beauty of this approach is of course that practically all kinds of beam profiles can be approximated by means of this method. However, from a theoretical point of view, the method is strictly only valid for beams that propagate in infinite space or at most perpendicular to any boundary. That is because integration is performed from $X = -\infty$ to $X = +\infty$ which is strictly only possible if space is uninterrupted in this interval. Therefore, if the oblique incidence is considered, the method is strictly wrong. Nevertheless, many authors apply the method even for oblique incidence. Furthermore, if large oblique incidence is considered for a narrow

beam, there is yet another difficulty which is again a consequence of the fact that the method is strictly only valid for normal incidence, and that is that “incident” infinite plane waves must be considered that are actually “coming from the continuing media.” This is of course a contradictive situation which is not present in the inhomogeneous waves decomposition of bounded beams (see below). Yet another important problem that arises if the Fourier method is applied is the fact that no inhomogeneous waves are present in the bounded beam under consideration. This may lead to wrong numerical simulations especially whenever complicated surfaces (for example corrugated surfaces) are considered.¹²⁻¹⁵ The reason is that inhomogeneous waves interact at interfaces differently from pure plane waves. This fact is very important because if one simulates a bounded inhomogeneous wave by means of the Fourier method, the resulting bounded beam may simulate reality incorrectly, especially in cases where rough surfaces are considered.¹²⁻¹⁵ That is the reason why this paper focuses on the description of bounded inhomogeneous waves in terms of infinite inhomogeneous plane waves.

IV. CLASSICAL GAUSSIAN BOUNDED BEAM FORMATION IN TERMS OF INFINITE INHOMOGENEOUS WAVES

The previous section suggests that it is not recommended to decompose a bounded inhomogeneous wave into

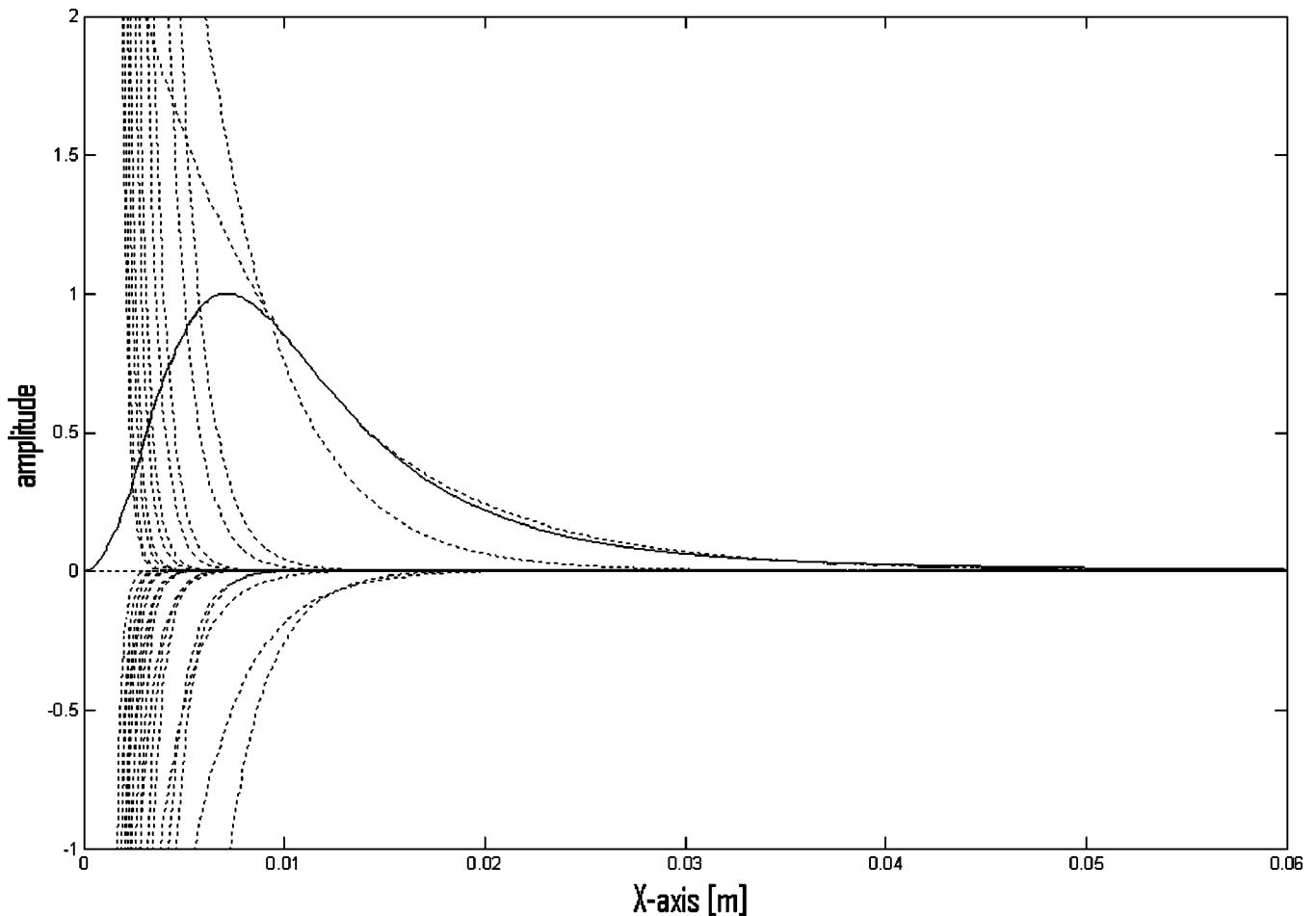


FIG. 6. Solid line: the exact profile (11). Dotted lines: the profiles of the infinite inhomogeneous waves that form the exact profile as in (13).

plane waves (Fourier method) because “contradictions” might occur and more importantly because the nature of plane waves is so different from that of (infinite) inhomogeneous (plane) waves that it is possible to perform the wrong simulations especially if the interaction is concerned with complicated interfaces such as periodically corrugated surfaces.^{12–15} Therefore it is necessary to focus on the decomposition of bounded beams by means of a superposition of infinite inhomogeneous plane waves. Several years ago Leroy *et al.*^{5–7} proposed such a method. The method consists of the formation of a bounded beam as a superposition of infinite inhomogeneous plane waves all propagating in the same direction, but having different amplitudes and inhomogeneities. Let us consider a beam with profile $f(x)$ which has to be decomposed as a superposition of inhomogeneous waves; then, if the sign convention (4) is adopted, one has⁵

$$f(x) = \sum_{n=0}^N A_n \exp(-\beta_n x). \quad (7)$$

Furthermore, one performs a coordinate transformation $x = p \ln y$ with $p \in \mathfrak{R}_0^+$ and $y \in (0, +\infty)$, whence, if $\beta_n = -n/p$,

$$\sum_{n=0}^N A_n y^n = f(p \ln y); \quad (8)$$

on the other hand, one applies a decomposition into Laguerre polynomials⁵ $L_n(y)$, such that

$$\sum_{n=0}^N B_n L_n(y) = f(p \ln y), \quad (9)$$

with

$$B_n = \int_0^{+\infty} \exp(-y) f(p \ln y) L_n(y) dy; \quad (10)$$

then the coefficients A_n in (7)–(8) are searched as a linear combination of B_i for $1 \leq i \leq N$. The drawback of this method is that (10) can only be found numerically, while the mentioned linear combination is not found straightforwardly but as an optimization procedure. The procedure is found to be best suited if Gaussian profiles are considered and is hence only applied for Gaussian beams or beam profiles that can be approximated by means of a small number of superposed Gaussian beams.^{5–7} Therefore, in what follows, we bring to light an analytical method that is valid for the kind of bounded beams $f(x)$ that is important in this report and is called “bounded inhomogeneous waves.”

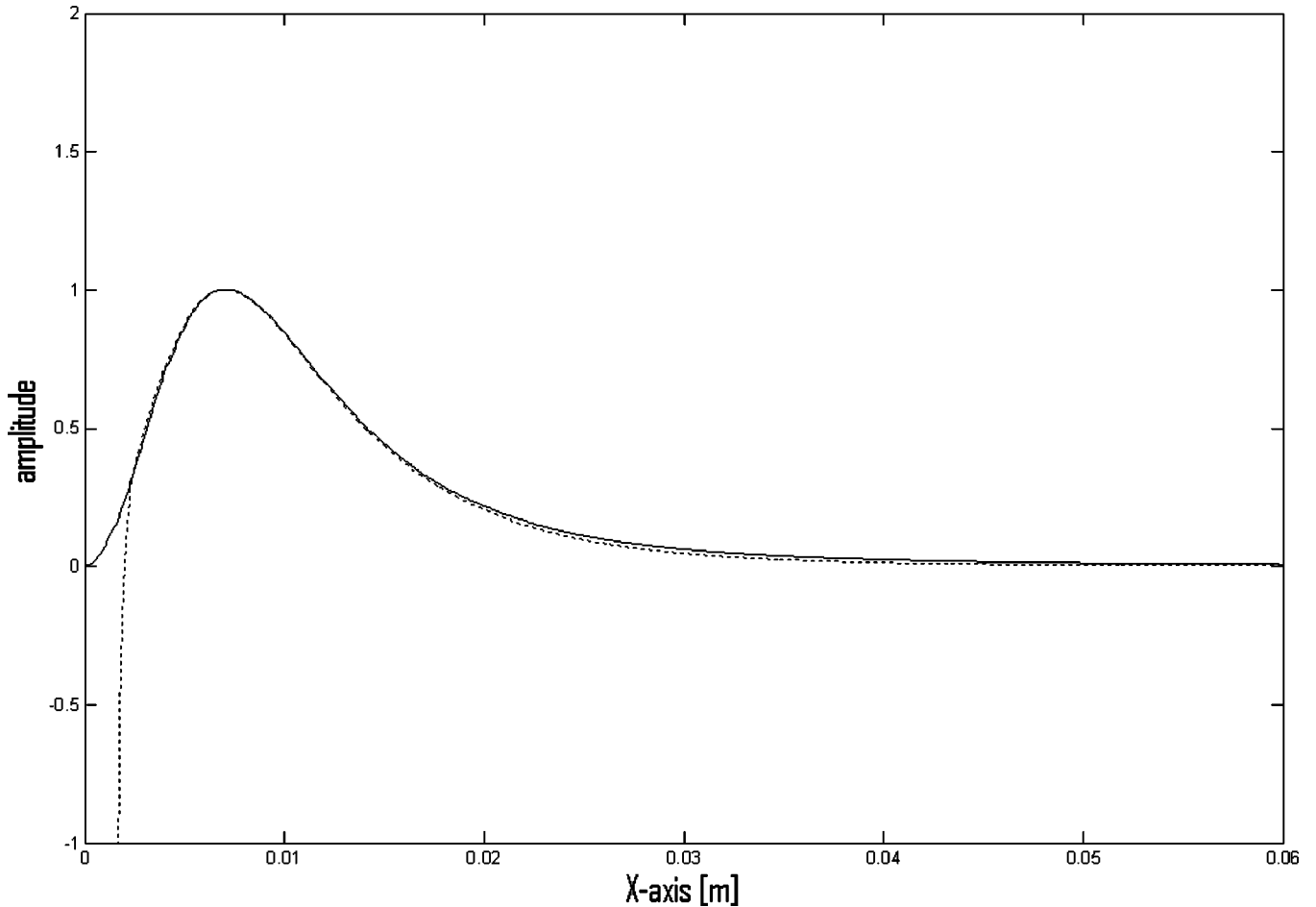


FIG. 7. Solid line: the exact profile (11). Dotted line: the summation of the inhomogeneous waves as in (13).

V. THE DESCRIPTION OF BOUNDED INHOMOGENEOUS WAVES BY MEANS OF THE LAPLACE TRANSFORM

A bounded inhomogeneous wave looks like an infinite inhomogeneous wave except for the important fact that it is chopped as a small interval in x -space. Hence it does not extend to infinity and is bounded in space. The main feature of such a bounded inhomogeneous wave is that it is exponentially shaped inside the beam and that its amplitude drops at the borders. Hence, depending on the method that is used to generate such waves, the shape at the borders may differ a bit, but the exponential feature remains unchanged. There are therefore many mathematical functions possible that describe the profile of a bounded beam. We have chosen a function for which an analytical solution exists for the amplitudes A_n in (7).

The profile of a bounded inhomogeneous wave, representing an exponentially decaying infinite inhomogeneous wave and traveling perpendicular to the x -axis, can sufficiently be described in the x -interval $[0, +\infty]$ by the analytical expression

$$f(x) = \frac{27W^4x^2}{4(x^2 + W^2)^3} \quad (11)$$

in which W is a parameter that is proportional to the “width”

of the beam profile. $f(x)$ reaches its maximum at

$$x_m = \frac{\sqrt{2}}{2} W. \quad (12)$$

Now, it would be possible to apply the numerical optimization technique of the previous section. However, it is here more convenient to apply an analytical approach. The first reason is that a numerical optimization procedure is far from natural and is in fact a fitting procedure. The expression “give me enough parameters and I will fit you an elephant” is perhaps most suitable to understanding the artificial character of any fitting procedure. The second reason is that it is known from experiments that bounded inhomogeneous waves behave like infinite inhomogeneous waves, therefore there must be a physical and an inherent analytical relation between the two kinds of waves.

Therefore we decompose $f(x)$ into decaying infinite inhomogeneous waves and we let the interval of the inhomogeneities β_n mathematically tend to infinity, while decreasing the distance between the successive inhomogeneities; hence

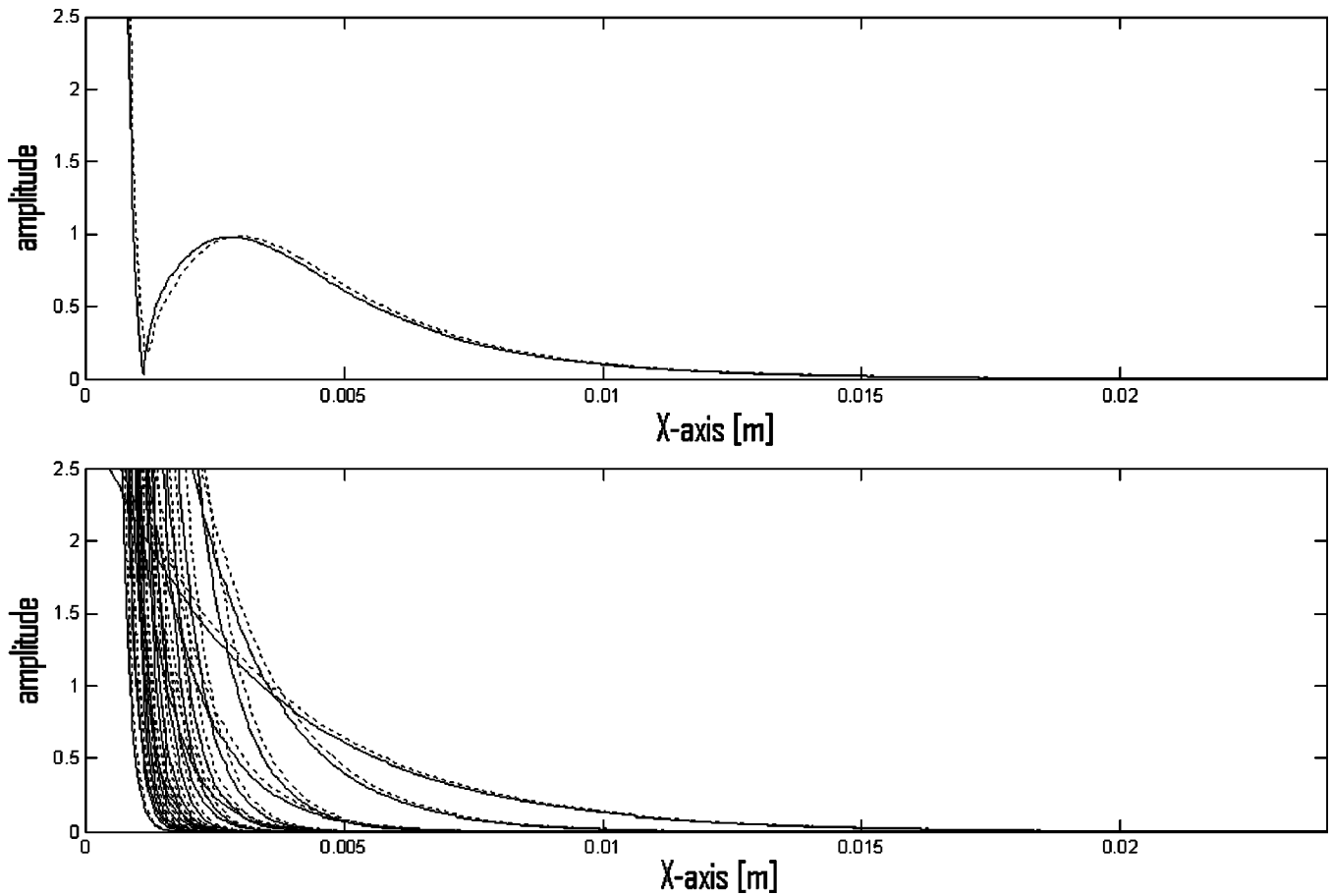


FIG. 8. Solid line: absolute value of the amplitude of the incident bounded inhomogeneous beam profile (top) and its infinite inhomogeneous waves building blocks (bottom). Dotted line: absolute value of the amplitude of the reflected bounded inhomogeneous beam profile (top) and its reflected infinite inhomogeneous waves building blocks (bottom). Inhomogeneity: 311.56/m. Angle of incidence: 30° (not in the vicinity of the Rayleigh angle).

$$f(x) = \sum_{n=0}^N B(-\beta_n) \exp(-\beta_n x) \\ \cong \int_0^{+\infty} e^{-\beta x} A(\beta) d\beta, \text{ with}$$

$$B(-\beta_n) = A(\beta_n) \Delta\beta_n. \quad (13)$$

The integral in (13) can be interpreted as the Laplace transform L of $A(\beta)$, therefore the unknown coefficients $A(\beta)$ can be obtained applying the inverse Laplace transform L^{-1} of the profile (11), thus releasing the problem of impractical numerical optimization procedures as they occur in the previous section. From textbooks containing tables of Laplace transforms, an analytical expression can be extracted,

$$A(\beta) = L^{-1}(f(x)) \\ = \frac{37W}{32} [(1 + W^2\beta^2) \sin(W\beta) - W\beta \cos(W\beta)]. \quad (14)$$

This is an oscillating function with increasing amplitude as a function of β , involving very high amplitudes attributed to very rapidly decreasing inhomogeneous waves. Therefore, high β values will only contribute to the amplitude near the origin, since their amplitude becomes negligible at larger distances. Still, in practice, we shall have to chop the integral

retaining a finite integration interval from $\beta=0$ to a chosen $\beta=\beta_{\max}$, whence the recovered bounded inhomogeneous wave profile will deviate considerably near $x=0$. The two reasons for this chop process are “numerical ease” and the requirement that \mathbf{k}_1 and \mathbf{k}_2 must be real, then considering (5) and (6) necessitates

$$\alpha \leq \alpha_0 \quad (15)$$

and

$$\beta^2 \leq \omega^2/v^2 - (\alpha_0)^2. \quad (16)$$

The second step is the re-discretization of the chopped integral in order to keep a finite number of infinite inhomogeneous waves forming the profile.

We therefore now examine the properties of the discrete and chopped summation of infinite inhomogeneous waves [see (13)] representing the bounded inhomogeneous wave as described in (11).

$$f(x) = \sum_{\beta=0}^{\beta_{\max}} A(\beta) \exp(-\beta) \Delta\beta. \quad (17)$$

It is always necessary to choose one value for W or, respectively, for β and then optimize the value of β , respectively, W in order to have the best agreement between the bounded inhomogeneous wave and the infinite inhomogeneous wave under consideration. As an example we consider the case

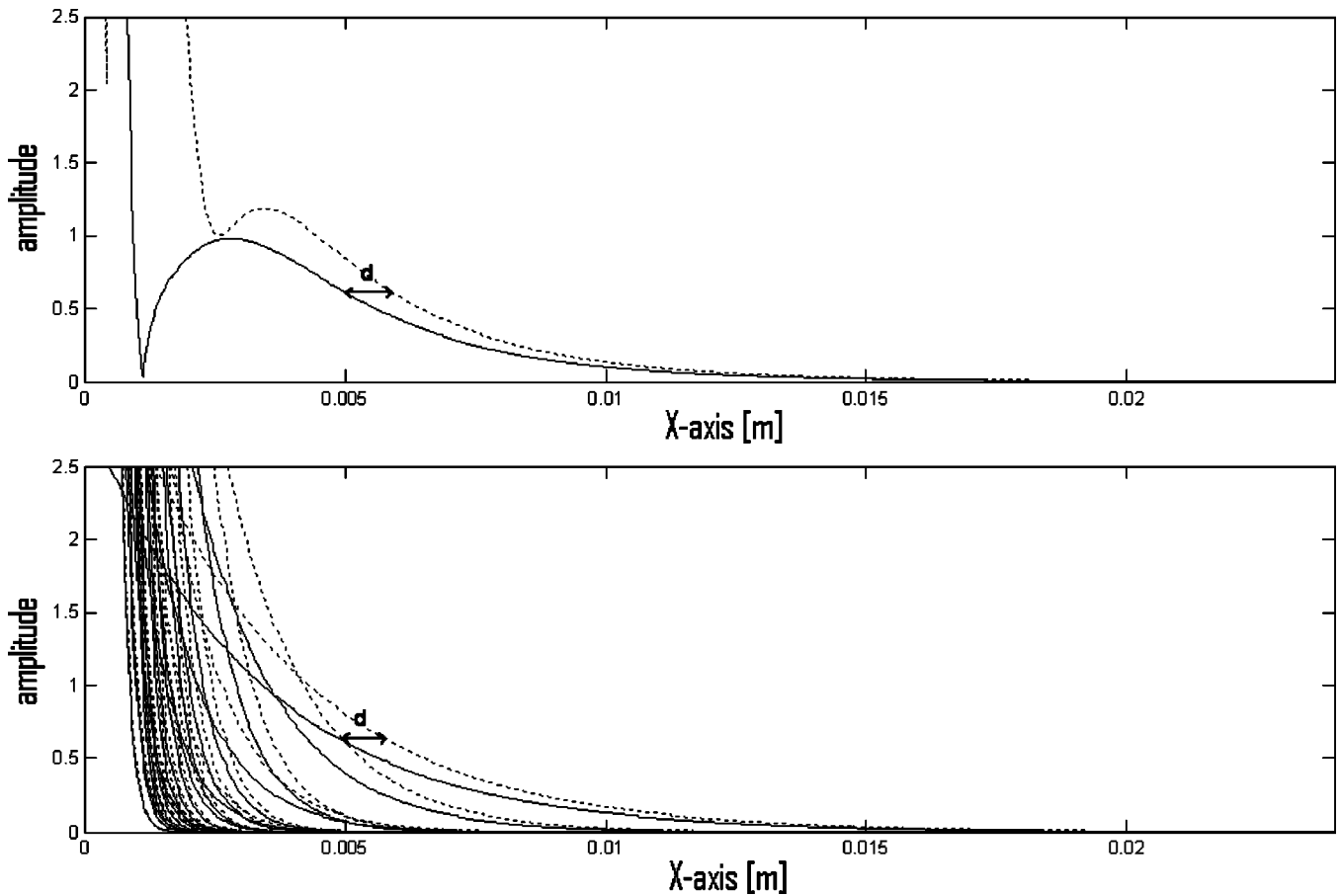


FIG. 9. Solid line: absolute value of the amplitude of the incident bounded inhomogeneous beam profile (top) and its infinite inhomogeneous waves building blocks (bottom). Dotted line: absolute value of the amplitude of the reflected bounded inhomogeneous beam profile (top) and its reflected infinite inhomogeneous waves building blocks (bottom). Inhomogeneity: $311.56/m$. Angle of incidence: 42° (in the neighborhood of the Rayleigh angle). It is seen that both the infinite and the bounded inhomogeneous wave are displaced by a distance d .

$W=0.01$ m. It is seen from Fig. 5 that the upper part of profile (11) can almost perfectly be approximated using one single inhomogeneous wave, having in this case an inhomogeneity $\beta=125/m$. This is as expected, since the profile (11) was made to locally represent an infinite inhomogeneous wave. If we need to approximate the complete profile (11), additional infinite inhomogeneous plane waves will be involved. In order to explain the behavior of a bounded inhomogeneous wave in the experiments cited above, we need to investigate the influence of the additional infinite inhomogeneous waves in the upper part of the bounded profile (11).

In Fig. 6, we have added each of the N terms in the summation (17) for $N=31$ and for $\beta_{\max}=3750/m$. The upper exponential is again the one for $\beta=125/m$. It is clear that this infinite inhomogeneous plane wave still dominates the upper part, i.e., for higher x values, of the bounded inhomogeneous wave (11). All other inhomogeneous waves dominate in the lower parts, i.e., for x values near zero, of the profile. That can explain why a bounded inhomogeneous wave in experiments behaves almost exactly (if the part of the beam near $X=0$ is not considered) as if it was an infinite inhomogeneous wave.

Next, in Fig. 7, all 31 inhomogeneous waves are summed to form the dashed line which is an approximation of the exact bounded inhomogeneous wave (solid line). A

considerable deviation occurs near the origin, as explained above.

VI. THE SCATTERING OF BOUNDED INHOMOGENEOUS WAVES

A. Theoretical development

We will now examine, by means of a numerical example, how a bounded inhomogeneous wave behaves during scattering at an interface between a liquid and an isotropic solid. We therefore highlight each individual incident infinite inhomogeneous wave and describe how it interacts with the interface.

Taking into account the generalized Snell–Descartes law (i.e., $k_x=k_x^{\text{inc}}$), we denote the potential for the incoming wave by

$$\varphi^{\text{inc}} = \exp i(k_x^{\text{inc}}x + k_z^{\text{inc}}z), \quad (18)$$

for the reflected wave by

$$\varphi^r = R \exp i(k_x^{\text{inc}}x + k_z^r z), \quad (19)$$

for the transmitted longitudinal wave by

$$\varphi^l = T_d \exp i(k_x^{\text{inc}}x + k_z^{ld}z), \quad (20)$$

and for the transmitted shear wave by

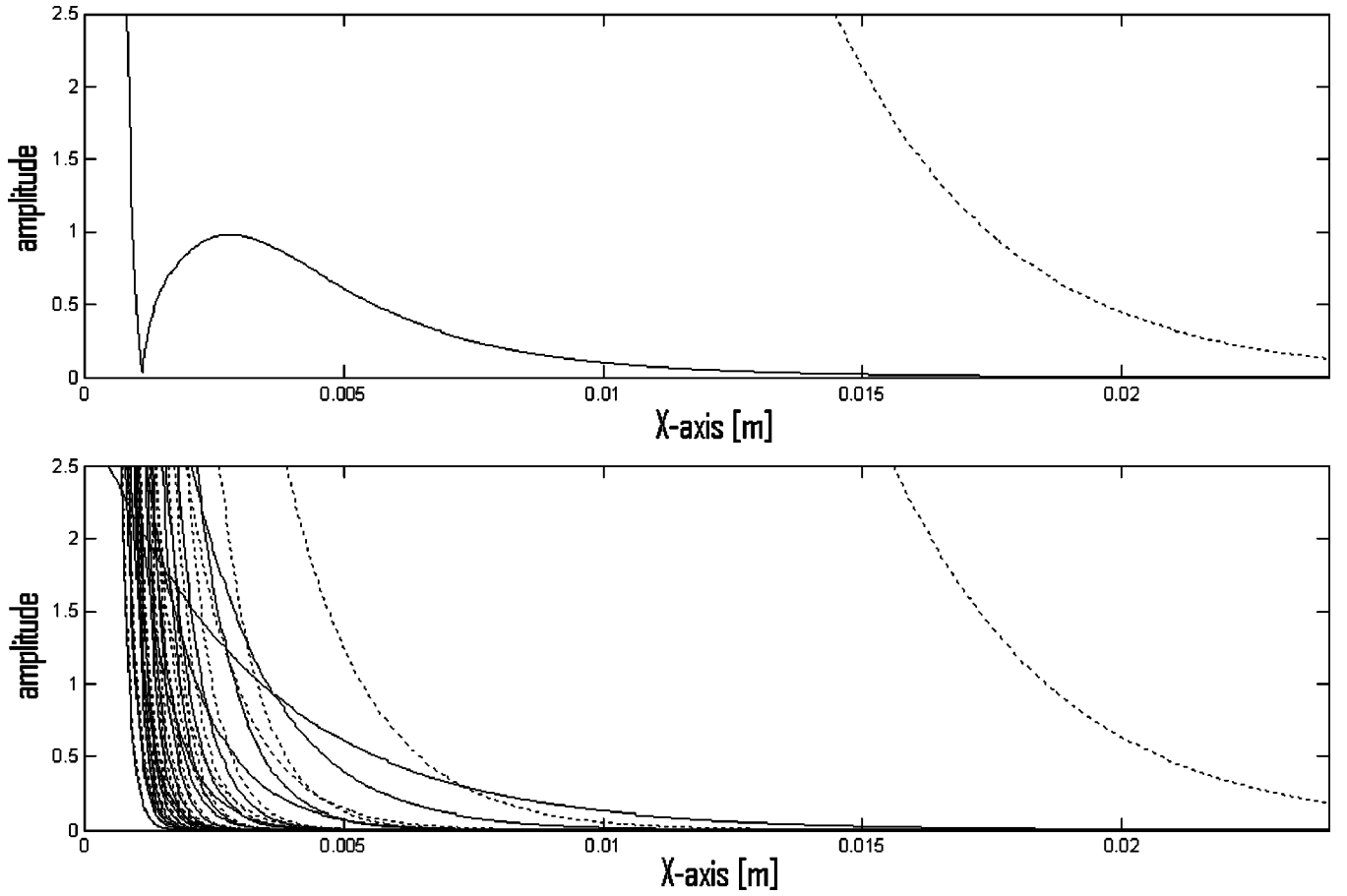


FIG. 10. Solid line: absolute value of the amplitude of the incident bounded inhomogeneous beam profile (top) and its infinite inhomogeneous waves building blocks (bottom). Dotted line: absolute value of the amplitude of the reflected bounded inhomogeneous beam profile (top) and its reflected infinite inhomogeneous waves building blocks (bottom). Inhomogeneity: 311.56/m. Angle of incidence: 44.045° (exactly the Rayleigh angle).

$$\psi = T_s \exp i(k_x^{\text{inc}} x + k_z^{\text{ts}} z) \mathbf{e}_y \quad (21)$$

where R is the reflection coefficient, T_d is the transmission coefficient for longitudinal waves and T_s is the transmission coefficient for shear waves. All wave vectors involved in (18)–(21) are supposed to be complex valued; cf. (3). Again we note that the sign of β is opposite to the one in Ref. 5, however, this is no problem because all the physics in the current paper is expressed in terms of \mathbf{k}_1 and \mathbf{k}_2 immediately. Taking into account (13), and taking into account the dispersion relation for inhomogeneous waves (2), we have

$$\begin{bmatrix} k_x^{\text{inc}} \\ k_z^{\text{inc}} \end{bmatrix} = \begin{bmatrix} \cos \theta^{\text{inc}} & \sin \theta^{\text{inc}} \\ -\sin \theta^{\text{inc}} & \cos \theta^{\text{inc}} \end{bmatrix} \begin{bmatrix} i\beta^{\text{inc}} \\ \sqrt{(\omega/\nu + i\alpha_0)^2 - (\beta^{\text{inc}})^2} \end{bmatrix} \quad (22)$$

and

$$k_z^r = \sqrt{(\omega/\nu + i\alpha_0)^2 - (k_x^{\text{inc}})^2}, \quad (23)$$

$$k_z^{\text{td}} = \sqrt{(\omega/\nu_d + i\alpha_{0d})^2 - (k_x^{\text{inc}})^2}, \quad (24)$$

$$k_z^{\text{ts}} = \sqrt{(\omega/\nu_s + i\alpha_{0s})^2 - (k_x^{\text{inc}})^2}. \quad (25)$$

In (22)–(25), ν is the wave velocity in the liquid, and ν_d and ν_s are the longitudinal, respectively, shear wave velocities in the solid.

The intrinsic damping coefficients in the liquid for longitudinal waves, respectively, in the solid for longitudinal

and shear homogeneous plane waves are denoted by α_0 , α_{0d} , and α_{0s} . For simplicity, we will suppose that there is no damping involved in our calculations.

We then develop the continuity conditions along the interface for normal displacements,

$$u_z^{\text{liquid}} = u_z^{\text{solid}}, \quad (26)$$

and for normal stress,

$$T_{p3}^{\text{liquid}} = T_{p3}^{\text{solid}}, \quad (27)$$

with

$$\mathbf{u}^{\text{liquid}} = \nabla(\varphi^{\text{inc}} + \varphi^r), \quad (28)$$

$$\mathbf{u}^{\text{solid}} = \nabla(\varphi^t) + \nabla \times \psi, \quad (29)$$

and

$$T_{pj}^q = \delta_{pj} \tilde{\lambda}^q \varepsilon_{rr}^q + 2\tilde{\mu}^q \varepsilon_{pj}^q, \quad (30)$$

in which we have used the Einstein double suffix notation convention, $q=1$ for the liquid and $q=2$ for the solid, and

$$\tilde{\lambda}^q = \lambda^q + i\omega\lambda'^q = \rho(\tilde{\nu}_d)^2, \quad (31)$$

$$\tilde{\mu}^q = \mu^q + i\omega\mu'^q = \rho \frac{(\tilde{\nu}_s)^2 - (\tilde{\nu}_d)^2}{2}, \quad (32)$$

$$\varepsilon_{kl}^q = \frac{1}{2} [\partial_l u_k^q + \partial_k u_l^q]. \quad (33)$$

The Lamé constants are denoted by λ and μ , while the viscoelastic damping coefficients are given by λ' and μ' . The

$$\begin{bmatrix} RD \\ T_D \\ T_S \end{bmatrix} = \begin{bmatrix} k_z^r & -k_z^{td} \\ 0 & -2k_z^{td} k_x^{\text{inc}} \\ -\tilde{\lambda}^1 \left(\frac{\omega}{\nu} + i\alpha_0 \right)^2 & \tilde{\lambda}^2 \left(\frac{\omega}{\nu_d} + i\alpha_{0d} \right)^2 + 2\tilde{\mu}^2 (k_z^{td})^2 \end{bmatrix}^{-1} \begin{bmatrix} -k_x^{\text{inc}} \\ \left(\frac{\omega}{\nu_s} + i\alpha_{0s} \right)^2 - 2(k_x^{\text{inc}})^2 \\ 2\tilde{\mu}^2 k_z^{ts} k_x^{\text{inc}} \end{bmatrix} \begin{bmatrix} -k_z^{\text{inc}} \\ \tilde{\lambda}^1 \left(\frac{\omega}{\nu} + i\alpha_0 \right)^2 \end{bmatrix}. \quad (34)$$

Remember that in order to obtain (34), we have incorporated the dispersion relation for inhomogeneous waves. Solving (34) requires proper choices of the signs of the z components of the wave vector. The latter can be found in the literature⁶ and is outlined in terms of \mathbf{k}_1 and \mathbf{k}_2 , i.e., independent of the choice of the sign of β in (4), as follows. The bulk critical angle for transmitted waves of type c ($c=s$ for shear, $c=d$ for longitudinal) is given by

$$\theta^c = \arcsin \frac{\nu}{\nu_c}. \quad (35)$$

Whenever $\theta^{\text{inc}} < \theta^c$, \mathbf{k}_1 , for that particular transmitted mode must point into the solid, which corresponds to the classical Sommerfeld conditions. Whenever $\theta^{\text{inc}} \geq \theta^c$, \mathbf{k}_2 , for that particular transmitted mode must point into the solid. For the reflected wave, it is always so that \mathbf{k}_1 must point into the liquid.

B. Numerical results

We consider a water/brass interface with $\nu = 1480$ m/s, $\nu_d = 4840$ m/s, $\nu_s = 2270$ m/s, $\rho_l = 1000$ kg/m³, $\rho_s = 8100$ kg/m³.

ρ_l , respectively, ρ_s are the densities of the liquid and the solid and are needed for the determination of the Lamé constants when applying the dispersion relation for inhomogeneous waves (2).

We know from calculations of the reflection coefficient by means of (34), involving inhomogeneous waves, that for 5 MHz, a Rayleigh wave is stimulated when $\theta^{\text{inc}} = 44.045^\circ$ and $\beta^{\text{inc}} = 311.56/\text{m}$, corresponding to the so called Rayleigh pole.

We thus consider a bounded inhomogeneous wave, having a Rayleigh wave stimulating inhomogeneity, i.e., $\beta = 311.56/\text{m} \Leftrightarrow W = 0.004$ m. We calculate the reflected profiles for different angles of incidence. All calculations are performed for $\beta_{\text{max}} = 6231.2$ and for 21 inhomogeneous waves with equidistant inhomogeneity coefficients $\beta \in [0, \beta_{\text{max}}]$. In Fig. 8, the angle of incidence θ^{inc} is 30° . This angle is far less than the Rayleigh angle. We notice that each infinite inhomogeneous wave by which the bounded inhomogeneous wave is built up, is shifted very little and so is the bounded inhomogeneous wave. In Fig. 9, the angle of inci-

definition of the “complex velocity $\bar{\nu}$ ” is found in (2), for the appropriate choice of shear or longitudinal wave material properties.

By applying the continuity conditions (26) and (27), we obtain

dence $\theta^{\text{inc}} = 42^\circ$, which is in the vicinity of the Rayleigh angle. We notice that the bounded inhomogeneous wave is shifted along the x -axis, by the same amount as its infinite inhomogeneous counterpart. At last, in Fig. 10 we have taken the exact Rayleigh angle of incidence $\theta^{\text{inc}} = 44.045^\circ$. We observe that both the bounded inhomogeneous wave and its infinite counterpart are shifted by almost the same distance along the interface. We must stress, however, that Figs. 5–10 cannot be used to check energy conservation, but solely to check displacement. The reason for that is the fact that the bounded inhomogeneous wave is written as a finite sum over a finite inhomogeneity interval. This causes deviations near $x=0$, therefore energy conservation cannot be checked. It is impossible to use the exact integral expression (13) without encountering numerical problems, otherwise such calculations would undoubtedly better involve the conservation of energy and hence limit the calculated intensities of the dotted line near $x=0$ in Fig. 10.

In contrast to bounded Gaussian beams, a bounded inhomogeneous wave does not cause a null zone or other peculiarities due to the Schoch effect. Hence nondestructive testing of materials using bounded inhomogeneous waves is quite different from the use of other types of bounded beams.

VII. CONCLUSIONS

We have presented the Laplace transform as a tool for analytically determining the unknown coefficients in the infinite inhomogeneous plane wave decomposition of a bounded inhomogeneous wave. We have also shown that it is understood from a theoretical point of view why in experiments bounded inhomogeneous waves behave almost as if they were infinitely extended. As an example, we have exposed how a bounded inhomogeneous wave is deformed after interaction with a water/brass interface and have verified that it is shifted in space by the same amount as its infinite inhomogeneous counterpart. This shift which is not really accompanied by a deformation is typical for bounded as well as for infinite inhomogeneous waves and differs much from strong deformations such as the well known Schoch effect for Gaussian beams.

ACKNOWLEDGMENTS

The authors are indebted to “The Flemish Institute for the Encouragement of the Scientific and Technological Research in Industry (I.W.T.)” for research support and to acknowledge the constructive suggestions and comments of the reviewers.

- ¹B. Poirée, “Plane evanescent waves in ideal liquids and elastic solids,” *J. Acoust.* **2**, 205–216 (1989).
- ²M. Deschamps, “The plane heterogeneous wave and its applications in linear acoustics,” *J. Acoust.* **4**, 269–305 (1991).
- ³B. Poirée, “Complex harmonic waves,” *Physical Acoustics*, edited by O. Leroy and M. A. Breazeale (Plenum, New York, 1991), pp. 99–117.
- ⁴G. Quentin, A. Derem, and B. Poirée, “The formalism of evanescent plane waves and its importance in the study of the generalized Rayleigh wave,” *J. Acoust.* **3**, 321–336 (1990).
- ⁵J. M. Claeys and O. Leroy, “Reflection and transmission of bounded sound beams on half spaces and through plates,” *J. Acoust. Soc. Am.* **72**, 585–590 (1982).
- ⁶K. Van Den Abeele and O. Leroy, “Complex harmonic wave scattering as the framework for investigation of bounded beam reflection and transmission at plane interfaces and its importance in the study of vibrational modes,” *J. Acoust. Soc. Am.* **93**, 308–323 (1993).
- ⁷K. Van Den Abeele and O. Leroy, “On the influence of frequency and width of an ultrasonic bounded beam in the investigation of materials: Study in terms of heterogeneous plane waves,” *J. Acoust. Soc. Am.* **93**, 2688–2699 (1993).
- ⁸M. Deschamps and B. Hosten, “The generation of bulk heterogeneous waves in a non-absorbing liquid,” *Acustica* **68**, 92–95 (1989).
- ⁹W. Huang, R. Briers, S. I. Rokhlin, and O. Leroy, “Experimental study of inhomogeneous wave reflection from a solid-air periodically rough boundary using leaky Rayleigh waves,” *J. Acoust. Soc. Am.* **96**, 363–369 (1994).
- ¹⁰M. Deschamps, “Reflection and refraction of the evanescent plane wave on plane interfaces,” *J. Acoust. Soc. Am.* **96**, 2841–2848 (1994).
- ¹¹R. Briers, O. Leroy, O. Poncelet, and M. Deschamps, “Experimental verification of the calculated diffraction field generated by inhomogeneous waves obliquely incident on a periodically rough liquid-solid boundary,” *J. Acoust. Soc. Am.* **106**, 682–687 (1999).
- ¹²N. F. Declercq, J. Degrieck, R. Briers, and O. Leroy, “Theoretical verification of the backward displacement of waves reflected from an interface having superimposed periodicity,” *Appl. Phys. Lett.* **82**, 2533–2534 (2003).
- ¹³N. F. Declercq, J. Degrieck, R. Briers, and O. Leroy, “A theoretical treatment of the backward beam displacement on periodically corrugated surfaces and its relation to leaky Scholte–Stoneley waves,” submitted elsewhere.
- ¹⁴N. F. Declercq, J. Degrieck, R. Briers, and O. Leroy, “A theoretical elucidation for the experimentally observed backward displacement of waves reflected from an interface having superimposed periodicity,” *J. Acoust. Soc. Am.* **112**, 2414 (2002).
- ¹⁵A. A. Teklu and M. A. Breazeale, “Backward displacement of ultrasonic waves reflected from a corrugated interface,” *J. Acoust. Soc. Am.* **113**, 2283–2284 (2003).